Eigenvalues and eigenvectors of banded Toeplitz matrices and the related symbols

S.-E. Ekström,[*1] and S. Serra-Capizzano,[†2,1]

[1]Department of Information Technology, Division of Scientific Computing, Uppsala University - ITC, Lägerhyddsv. 2, hus 2, P.O. Box 337, SE-751 05, Uppsala (SWEDEN)

[2]Department of Science and high Technology, Insubria University - via Valleggio 11, 22100 Como (ITALY)

May 15, 2017

Abstract

It is known that for the tridiagonal Toeplitz matrix, having the main diagonal with constant $a_0 = 2$ and the two first off-diagonals with constants $a_1 = -1$ (lower) and $a_{-1} = -1$ (upper), there exists closed form formulas, giving the eigenvalues of the matrix and a set of associated eigenvectors. The latter matrix corresponds to the well known case of the 1D discrete Laplacian, but with a little care the formulas can be generalized to any triple (a_0, a_1, a_{-1}) of complex values.

In the first part of this article, we consider a tridiagonal Toeplitz matrix of the same form $(a_0, a_\omega, a_{-\omega})$, but where the two off-diagonals are positioned ω steps from the main diagonal instead of only one. We show that its eigenvalues and eigenvectors also can be identified in closed form. To achieve this, ad hoc sampling grids have to be considered, in connection with a new symbol associated with the standard Toeplitz generating function. In the second part, we restrict our attention to the symmetric real case ($a_0, a_\omega = a_{-\omega}$ real values) and we analyze the relations with the standard generating function of the Toeplitz matrix. Furthermore, as numerical evidences clearly suggest, it turns out that the eigenvalue behavior of a general banded symmetric Toeplitz matrix with real entries can be described qualitatively in terms of that of the symmetrically sparse tridiagonal case with real a_0, $a_\omega = a_{-\omega}$, $\omega = 2, 3, \ldots$, and also quantitatively in terms of that having monotone symbols, as those related to classical Finite Difference discretization of the operators $(-1)^q \frac{\partial^{2q}}{\partial x^{2q}}$, where the case of $q = 1$ coincides with $a_0 = 2$, $a_1 = a_{-1} = -1$.

1 Introduction

Let A_n be a Toeplitz matrix of order n and let $\omega < n$ be a positive integer,

$$A_n = \begin{bmatrix} a_0 & \cdots & a_{-\omega} & & & \\ \vdots & \ddots & & \ddots & & \\ & & \ddots & & \ddots & \\ a_\omega & & \ddots & & \ddots & \\ & \ddots & & \ddots & & a_{-\omega} \\ & & \ddots & & \ddots & \vdots \\ & & & a_\omega & \cdots & a_0 \end{bmatrix}, \tag{1}$$

where the coefficients a_k, $k = -\omega, \ldots, \omega$, are complex numbers.

Let $f \in L^1(-\pi, \pi)$ and let $T_n(f)$ be the Toeplitz matrix generated by f i.e. $(T_n(f))_{s,t} = \hat{f}_{s-t}$, $s, t = 1, \ldots, n$, with f being the generating function of $\{T_n(f)\}$ and with $\hat{f}_k$ being the k-th Fourier coefficient of f, that is

$$\hat{f}_k = \frac{1}{2\pi} \int_{-\pi}^{\pi} f(\theta)\, e^{-\mathbf{i}k\theta}\, \mathrm{d}\theta, \quad \mathbf{i}^2 = -1, \quad k \in \mathbb{Z}. \tag{2}$$

If f is real-valued then several spectral properties are known (localization, extremal behavior, collective distribution) (see [7, 15] and references therein) and f is also the spectral symbol of $\{T_n(f)\}$ in the Weyl sense [7, 13, 20, 21]. If f is complex-valued, then the same type of information is transferred to the singular values, while the eigenvalues can have a 'wild' behavior [17] in some cases. According to the notation above, our setting is very special since by direct computation the generating function of the Toeplitz matrix in (1) is the function $f(\theta)$, a trigonometric polynomial defined as $\sum_{k=-\omega}^{\omega} a_k e^{\mathbf{i}k\theta}$, that is $A_n = T_n(f)$.

[*]sven-erik.ekstrom@it.uu.se

[†]s.serracapizzano@uninsubria.it

In this paper we are interested in the quantitative estimates of the eigenvalues of A_n. Indeed, in the the band symmetric Toeplitz setting, quantitative estimates are already available in the relevant literature. In fact, using an embedding argument in the Tau algebra (the set of matrices diagonalized by a sine transform, [1]), we are lead to the conclusion that the j-th eigenvalue $\lambda_j(T_n(f)) = \lambda_{j,n}$ of a real symmetric matrix A_n, and the eigenvalues of $T_n(f)$ are sorted in a non-decreasing order, as in (1), but with $a_k = a_{-k} \in \mathbb{R}$, $k = 1, \ldots, \omega$, can be approximated by the value $f(\theta_{j,n})$ with an error bounded by $K_f h$, where K_f is a constant depending on f, but independent of h and j (see [1, 3, 9, 10, 16] and references therein).

The following notation is used throughout this paper. With a θ we mean a classical equispaced grid; defined for a given n the grid the points $\theta_{j,n} = \frac{j\pi}{n+1}$. The full grid is denoted $\theta_n = \{\theta_{j,n}\}$. In the same manner we denote by $\tilde{\theta}$ the new grid defined in Section 2 if this article. When adding a third subscript, r, we mean the r:th repetition of j:th grid point, that is $\theta_{r,j,n}$ is the same for all r with fixed j and n. By λ_n we denote the sorted eigenvalues (non-decreasing order). By μ_n we denote the unsorted eigenvalues using the new grid. By ν_n we denote the unsorted eigenvalue approximations from standard grid and standard symbol, and ξ_n denotes the sorted approximations (non-decreasing order).

Here, taking into account the notation above, we furnish more precise estimates in some cases and we discuss the general setting, as explained in the following.

More specifically, in Section 2, we consider the special case where a_0, a_ω, $a_{-\omega} \in \mathbb{C}$, $a_k = 0$ for $k \neq 0, \pm\omega$ (the nontrivial setting is when $a_\omega a_{-\omega} \neq 0$). Under such assumptions, starting from the generating function $f(\theta) = a_0 + a_\omega e^{\mathbf{i}\omega\theta} + a_{-\omega} e^{-\mathbf{i}\omega\theta}$ and from a grid $\tilde{\theta}_n = \{\tilde{\theta}_{j,n}\}$ where $j = 1, \ldots, n$ described in Subsection 2.1, we give the closed form expression of the eigenvalues and eigenvectors in Subsection 2.2: a new simplified symbol emerges since the eigenvalues $\mu_n = \{\mu_{j,n}\}$, where $j = 1, \ldots, n$, are exactly given as $\mu_{j,n} = g\left(\tilde{\theta}_{j,n}\right)$, with $\tilde{\theta}_n$ a proper grid on $[0, \pi]$ and $g(\theta) = a_0 + 2\sqrt{a_\omega a_{-\omega}}\cos(\theta)$, where the new symbol $g(\theta)$ is different from the generating function $f(\theta) = a_0 + a_\omega e^{\mathbf{i}\omega\theta} + a_{-\omega} e^{-\mathbf{i}\omega\theta}$ and does not depend on ω, while the grid $\tilde{\theta}_n$ contains the information on ω. Finally, in Subsection 2.3, we discuss few relationships between the symbol g and the generating function f, in terms of the concepts of re-arrangement (see e.g. [19] and references therein) and of spectral symbol in the Weyl sense.

In Section 3 we impose real symmetry to the matrices (1) and we consider different cases. More in detail, in Subsection 3.1, we assume that only nonzero real coefficients of (1) are a_0 and $a_\omega = a_{-\omega}$. We compare the true eigenvalues $\lambda_{j,n}$, $j = 1, \ldots, n$, sorted in a non-decreasing order, with the generating function $f(\theta) = a_0 + 2a_\omega \cos(\omega\theta)$ evaluated at the grid given by the points $\frac{j\pi}{n+1}$, that is not an exact approximation (except for $\omega = 1$). Since a closed form symbol and grid for the exact evaluation of the eigenvalues are given in Theorem 1, the algorithm to approximate the expansion of the error, given in [9], is examined.

For any given sequence of indices n, where $\beta = \mathrm{mod}(n, \omega)$, $\beta = 0, 1, \ldots, \omega - 1$, we show numerically that ω different "error modes" emerges, and hence in total ω^2 different "error modes" can be observed for a symbol of the type $f(\theta) = a_0 + 2a_\omega \cos(\omega\theta)$.

We show that each error mode $s = 0, \ldots, \omega - 1$, of a given β, has the form

$$E^{\{s\}}_{j_\omega, n_\omega + \eta} = \lambda_{j_s,n} - f\left(\theta_{\sigma_n(j_s),n}\right) = \sum_{k=1}^{\infty} c_{k,s}\left(\theta_{\sigma_n(j_s),n}\right) h^k, \qquad h = \frac{1}{n+1}$$

and present analytical and numerical results regarding $c_{k,s}(\theta)$: see (48) and (49) for the formal definition of all variables.

On the other hand, when considering the Finite Difference approximation of the operators $(-1)^q \frac{\partial^{2q}}{\partial x^{2q}}$, $q \geq 1$,we obtain Toeplitz matrices $T_n(f)$ with $f(\theta) = (2 - 2\cos(\theta))^q$ (the case of $q = 1$ coincides with $a_0 = 2$, $a_\omega = a_{-\omega} = -1$, $\omega = 1$). In such a case with $q > 1$, and more generally for monotone symbols f, the error below has the form

$$E_{j,n} = \lambda_{j,n} - f(\theta_{j,n}) = \sum_{k=1}^{\infty} c_k(\theta_{j,n}) h^k, \qquad h = \frac{1}{n+1}, \tag{3}$$

with $\theta_{j,n} = j\pi h, j = 1, \ldots, n$, and $c_k(\theta)$, $k = 1, 2, \ldots$, higher order symbols (regarding (3), see the algorithmic proposals and related numerics in [9, 10] and the analysis in [4]).

The functions $c_{k,s}(\theta)$ and $c_k(\theta)$ can be approximated and a scheme is presented for performing such computations. When f is a cosine trigonometric polynomial monotone on $[0, \pi]$, we have to mention that in [2, 5] expansions as in (3) are in part formally proven: however, one of the assumptions, that is the positivity of the second derivative at zero (see [2][page 310, line 3]), excludes the important case of Finite Difference approximations of (high order) differential operators considered here since $f(\theta) = (2 - 2\cos(\theta))^q$, while the given expansions, as shown in [9], can be exploited for designing fast eigensolvers for large matrices.

In Subsection 3.2, we analyze the case of the general matrices in (1) with a_k are real with $a_k = a_{-k}$, $k = 1, \ldots, \omega$. We consider the features and behavior of the error of the eigenvalue approximation using the symbol, since here a grid and a function giving the exact eigenvalues are not known. However, we show

numerically that the eigenvalue behavior of a general banded symmetric Toeplitz matrix with real entries can be described, qualitatively in terms of that of the symmetrically sparse tridiagonal (SST) case with real a_0, $a_\omega = a_{-\omega}$, $\omega = 2, 3, \ldots$, and also quantitatively in terms of that having monotone symbols as those related to the classical Finite Difference discretization of the operators $(-1)^q \frac{\partial^{2q}}{\partial x^{2q}}$, $q \in \mathbb{N}$, $q \neq 0, 1$.

Some conclusions and possible directions of extending the current results are given in Section 4.

2 Exact eigenvalues and eigenvectors of SST complex valued Toeplitz matrices and the related symbols

Let A_n be a Toeplitz matrix of order n and with the following nonzero structure

$$A_n = \begin{bmatrix} a_0 & \overbrace{0 & \cdots & 0}^{\omega-1} & a_{-\omega} & & \\ 0 & a_0 & \ddots & \ddots & \ddots & \ddots & \\ \vdots & \ddots & \ddots & \ddots & \ddots & \ddots & a_{-\omega} \\ 0 & \ddots & \ddots & \ddots & \ddots & \ddots & 0 \\ a_\omega & \ddots & \ddots & \ddots & \ddots & \ddots & \vdots \\ & \ddots & \ddots & \ddots & \ddots & a_0 & 0 \\ & & a_\omega & 0 & \ldots & 0 & a_0 \end{bmatrix}, \tag{4}$$

where the constant coefficients $a_0, a_\omega, a_{-\omega}$ can be real or complex. The constants a_ω and $a_{-\omega}$ are located on the $\omega, -\omega$ off-diagonals, respectively. The generating function for the matrix $A_n = T_n(f)$ is defined as

$$f(\theta) = a_0 + a_\omega e^{\mathbf{i}\omega\theta} + a_{-\omega} e^{-\mathbf{i}\omega\theta} \tag{5}$$

which is also the symbol of the sequence of matrices $\{A_n = T_n(f)\}$ in the Weyl sense [7, 13, 20, 21]. Notably, when $a_\omega a_{-\omega} \neq 0$, the matrix A_n can be symmetrized in the sense that there exists a diagonal invertible matrix D_n such that

$$A_n^{\text{sym}} = D_n A_n D_n^{-1} = \begin{bmatrix} a_0 & \overbrace{0 & \cdots & 0}^{\omega-1} & \sqrt{a_\omega a_{-\omega}} & & \\ 0 & a_0 & \ddots & \ddots & \ddots & \ddots & \\ \vdots & \ddots & \ddots & \ddots & \ddots & \ddots & \sqrt{a_\omega a_{-\omega}} \\ 0 & \ddots & \ddots & \ddots & \ddots & \ddots & 0 \\ \sqrt{a_\omega a_{-\omega}} & \ddots & \ddots & \ddots & \ddots & \ddots & \vdots \\ & \ddots & \ddots & \ddots & \ddots & a_0 & 0 \\ & & \sqrt{a_\omega a_{-\omega}} & 0 & \ldots & 0 & a_0 \end{bmatrix}. \tag{6}$$

Therefore, A_n and A_n^{sym} are similar and share the same eigenvalues, where $A_n^{\text{sym}} = T_n(g_\omega)$ with

$$g_\omega(\theta) = a_0 + 2\sqrt{a_\omega a_{-\omega}} \cos(\omega\theta). \tag{7}$$

For the particular case $\omega = 1$, by defining the equidistant grid

$$\theta_{j,n} = \frac{j\pi}{n+1} = j\pi h, \quad j = 1, \ldots, n, \quad h = \frac{1}{n+1}, \tag{8}$$

the j-th eigenvalue $\mu_{j,n}$ [1, 6, 11, 12, 14, 18] of A_n is known in closed form, expressed as

$$\mu_{j,n} = a_0 + 2\sqrt{a_\omega a_{-\omega}} \cos(\theta_{j,n}), \quad j = 1, \ldots, n. \tag{9}$$

We notice that $\mu_{j,n} = g(\theta_{j,n})$ with $g(\theta) = g_1(\theta) = a_0 + 2\sqrt{a_1 a_{-1}} \cos(\theta)$, for g_ω with $\omega = 1$ given in equation (7).

Furthermore, for the eigenvalue $\mu_{j,n}$, a corresponding eigenvector $\mathbf{x}_{j,n} = \left[x_1^{(j,n)}, \ldots, x_n^{(j,n)}\right]^{\mathrm{T}}$ has components given as follows

$$x_k^{(j,n)} = \left(\sqrt{\frac{a_\omega}{a_{-\omega}}}\right)^k \sin(k\theta_{j,n}), \quad k = 1, \ldots, n. \tag{10}$$

We introduce now a new sampling grid, $\tilde{\theta}_n$, which gives the exact eigenvalues $\mu_{j,n}$ for any $a_0, a_\omega, a_{-\omega} \in \mathbb{C}$ and $\omega \in \mathbb{N}, \omega < n$, in (9), and we introduce a modified version of (10) for expressing the corresponding eigenvectors $\mathbf{x}_{j,n}$.

2.1 The new sampling grid

We start by introducing a new grid $\tilde{\theta}_n$, defined in the subsequent scheme. We first define β as the remainder of the Euclidian division of n by ω, that is

$$\beta = n - \omega n_\omega \quad 0 \leq \beta < n, \quad n, \omega, \beta, n_\omega \in \mathbb{N}, \tag{11}$$

or, in other words, β is the modulus operator applied to the pair (n, ω), $\beta = \mathrm{mod}(n, \omega)$, and n_ω is the quotient i.e.

$$n_\omega = \frac{n - \beta}{\omega}, \tag{12}$$

which will be used as a "new" n in the subsequent definition of the new grid. We then construct two separate grids, each with a standard equidistant sampling, expressed as

$$\theta_{j_1, n_\omega} = \frac{j_1 \pi}{n_\omega + 1}, \quad j_1 = 1, \ldots, n_\omega, \tag{13}$$

$$\theta_{j_2, n_\omega + 1} = \frac{j_2 \pi}{n_\omega + 2}, \quad j_2 = 1, \ldots, n_\omega + 1. \tag{14}$$

We know that there might be multiple eigenvalues of multiplicity greater than one, and thus we might need to repeat the same grid point multiple times. Hence, we set the following gridpoints

$$\tilde{\theta}^{(1)}_{r_1, j_1, n_\omega(\omega - \beta)} = \theta_{j_1, n_\omega}, \qquad r_1 = 1, \ldots, \omega - \beta, \quad j_1 = 1, \ldots, n_\omega, \tag{15}$$

$$\tilde{\theta}^{(2)}_{r_2, j_2, (n_\omega + 1)\beta} = \theta_{j_2, n_\omega + 1}, \qquad r_2 = 1, \ldots, \beta, \quad j_2 = 1, \ldots, n_\omega + 1, \tag{16}$$

which is the same as writing that the grid points in (13) are repeated $\omega - \beta$ times and the grid points in (14) are repeated β times. Now define the following two grids

$$\tilde{\theta}^{(1)}_{n_\omega(\omega - \beta)} = \left\{ \left\{ \tilde{\theta}^{(1)}_{r_1, j_1, n_\omega(\omega - \beta)} \right\}_{r_1 = 1}^{\omega - \beta} \right\}_{j_1 = 1}^{n_\omega}, \tag{17}$$

$$\tilde{\theta}^{(2)}_{(n_\omega + 1)\beta} = \left\{ \left\{ \tilde{\theta}^{(2)}_{r_2, j_2, (n_\omega + 1)\beta} \right\}_{r_2 = 1}^{\beta} \right\}_{j_2 = 1}^{n_\omega + 1}. \tag{18}$$

The full sampling grid $\tilde{\theta}_n$ is finally given by the union of the two grids (17) and (18)

$$\tilde{\theta}_n = \tilde{\theta}^{(1)}_{n_\omega(\omega - \beta)} \bigcup \tilde{\theta}^{(2)}_{(n_\omega + 1)\beta}. \tag{19}$$

Example 1. *In order to illustrate the process a simple example is given. Take $n = 5$ and $\omega = 3$, then $\beta = 2$ and $n_\omega = 1$. Thus, by* (13) *and* (14) *we have $j_1 = 1$ and $j_2 = 1, 2$,*

$$\theta_{1,1} = \frac{\pi}{2}, \quad \theta_{1,2} = \frac{\pi}{3}, \quad \theta_{2,2} = \frac{2\pi}{3}.$$

Since $\omega - \beta = 1$ and $\beta = 2$, $\theta_{1,1}$ occurs only once and $\theta_{1,2}$ and $\theta_{2,2}$ are both repeated twice, that is (17) *and* (18) *are*

$$\tilde{\theta}^{(1)}_1 = \left\{ \frac{\pi}{2} \right\}, \quad \tilde{\theta}^{(2)}_4 = \left\{ \frac{\pi}{3}, \frac{\pi}{3}, \frac{2\pi}{3}, \frac{2\pi}{3} \right\}.$$

Consequently, the full grid $\tilde{\theta}_5$ of (19) *is expressed as*

$$\tilde{\theta}_5 = \left\{ \frac{\pi}{2}, \frac{\pi}{3}, \frac{\pi}{3}, \frac{2\pi}{3}, \frac{2\pi}{3} \right\}.$$

If the eigenvectors have to be expressed analytically, the latter grid should remain in this form (or retain information on the rearrangement if the gridpoints are rearranged): see Theorem 2.

2.2 Eigenvalues and eigenvectors described by the new sampling grid

We start with the main results.

Theorem 1. *The eigenvalues of a SST Toeplitz matrix with center diagonal a_0 and two off-diagonals a_ω and $a_{-\omega}$ at off-diagonal $-\omega$ and ω, as in (4), are given by*

$$\mu_{j,n} = g\left(\tilde{\theta}_{j,n}\right) = a_0 + 2\sqrt{a_\omega a_{-\omega}}\cos\left(\tilde{\theta}_{j,n}\right), \quad j = 1, \ldots, n, \tag{20}$$

where $\tilde{\theta}_{j,n}$ is the j-th component of the grid $\tilde{\theta}_n$ defined in (19).

Remark 1. *By $\mu_n^{(1)}$ and $\mu_n^{(2)}$ we denote the eigenvalues given by the symbol evaluations of grids $\tilde{\theta}^{(1)}_{n_\omega(\omega-\beta)}$ and $\tilde{\theta}^{(2)}_{(n_\omega+1)\beta}$ given in* (17) *and* (18)*. Assume $a_\omega a_{-\omega} \geq 0$ so that $g(\cdot)$ is real-valued, let $\lambda_{j,n}$ be the eigenvalues $\mu_{j,n}$ in Theorem 1 sorted in a non-decreasing order, and let π_n be a permutation of $\{1, \ldots, n\}$ which sorts the samples $g(\tilde{\theta}_{1,n}), \ldots, g(\tilde{\theta}_{n,n})$ in nondecreasing order i.e. $g(\tilde{\theta}_{\pi_n(1),n}) \leq \ldots \leq g(\tilde{\theta}_{\pi_n(n),n})$. Then*

$$\lambda_{j,n} = g\left(\tilde{\theta}_{\pi_n(j),n}\right) \quad j = 1, \ldots, n,$$

Theorem 2. *Given a SST Toeplitz matrix with center diagonal a_0 and two off-diagonals a_ω and $a_{-\omega}$ at off-diagonal $-\omega$ and ω, as in (4), the following statements concerning its eigenvalues and eigenvectors hold.*

For each eigenvalue given by $\mu^{(1)}_{r_1,j_1,n_\omega(\omega-\beta)} = g\left(\tilde{\theta}^{(1)}_{r_1,j_1,n_\omega(\omega-\beta)}\right) = g\left(\theta_{j_1,n_\omega}\right)$ with $j_1 = 1, \ldots, n_\omega$, and $r_1 = 1, \ldots, \omega - \beta$ we define a corresponding eigenvector $\mathbf{x}^{(1)}_{r_1,j_1,n} = \left[x_1^{(r_1,j_1,n)}, \ldots, x_n^{(r_1,j_1,n)}\right]^{\mathrm{T}}$, with components

$$x^{(r_1,j_1,n)}_{\omega(k_1-1)+r_1+\beta} = \left(\sqrt{\frac{a_\omega}{a_{-\omega}}}\right)^{k_1} \sin\left(k_1\theta_{j_1,n_\omega}\right), \quad k_1 = 1, \ldots, n_\omega, \tag{21}$$

and all non-defined components of $\mathbf{x}_{r_1,j_1,n}$ equal to zero.

For each eigenvalue $\mu^{(2)}_{r_2,j_2,(n_\omega+1)\beta} = g\left(\tilde{\theta}^{(2)}_{r_2,j_2,(n_\omega+1)\beta}\right) = g\left(\theta_{j_2,n_\omega+1}\right)$ with $j_2 = 1, \ldots, n_\omega + 1$, and $r_2 = 1, \ldots, \beta$ we can define a corresponding eigenvector $\mathbf{x}^{(2)}_{r_2,j_2,n} = \left[x_1^{(r_2,j_2,n)}, \ldots, x_n^{(r_2,j_2,n)}\right]^{\mathrm{T}}$, where the components are

$$x^{(r_2,j_2,n)}_{\omega(k_2-1)+r_2} = \left(\sqrt{\frac{a_\omega}{a_{-\omega}}}\right)^{k_2} \sin\left(k_2\theta_{j_2,n_\omega+1}\right), \quad k_2 = 1, \ldots, n_\omega + 1, \tag{22}$$

and all non defined components of $\mathbf{x}_{r_2,j_2,n}$ are equal to zero.

Remark 2. *To save memory and evaluations, the steps to construct $\tilde{\theta}_n$ defined in (2.1), after* (13) *and* (14)*, can of course be skipped, as long as information concerning recurring eigenvalues is stored. Note that if a grid is desired with all $\theta \in \tilde{\theta}_n$ unique in $[0, \pi]$, one can modify the set $\tilde{\theta}_n$ in* (19) *as follows: take $\theta \in \tilde{\theta}_n/\omega$ and then shift each grid point by appropriate multiples of π/ω. Then also the symbol reported in Theorem 1 has to be modified and instead of $g(\theta) = g_1(\theta)$ we use the generating function of the symmetrized matrix A_n^{sym} that is $g_\omega(\theta) = a_0 + 2\sqrt{a_\omega a_{-\omega}}\cos(\omega\theta)$. In Example 1 the grid is then for example $\tilde{\theta}_5 = \left\{\frac{\pi}{9}, \frac{2\pi}{9}, \frac{\pi}{2}, \frac{7\pi}{9}, \frac{8\pi}{9}\right\}$.*

Proof of Theorem 1 and Theorem 2 The proof for $\omega > 1$ follows the same ideas as for the case $\omega = 1$ presented in [6]. We start by observing that the matrix A_n in (4) has the standard symbol

$$f(\theta) = a_0 + a_\omega e^{\mathbf{i}\omega\theta} + a_{-\omega}e^{-\mathbf{i}\omega\theta}.$$

and assuming $a_\omega \neq 0$ and $a_{-\omega} \neq 0$, and define $\gamma = \sqrt{\frac{a_{-\omega}}{a_\omega}}$ we consider the following matrix B_n as follows

$$B_n = \begin{bmatrix} 0 & \overbrace{0 & \cdots & 0}^{\omega-1} & \gamma^2 & & \\ 0 & 0 & \ddots & \ddots & \ddots & \ddots & \\ \vdots & \ddots & \ddots & \ddots & \ddots & \ddots & \gamma^2 \\ 0 & \ddots & \ddots & \ddots & \ddots & \ddots & 0 \\ 1 & \ddots & \ddots & \ddots & \ddots & \ddots & \vdots \\ & \ddots & \ddots & \ddots & \ddots & 0 & 0 \\ & & 1 & 0 & \ldots & 0 & 0 \end{bmatrix},$$

Then B_n has the symbol

$$f_B(\theta) = e^{\mathbf{i}\omega\theta} + \gamma^2 e^{-\mathbf{i}\omega\theta} = e^{\mathbf{i}\omega\theta} + \frac{a_{-\omega}}{a_\omega} e^{-\mathbf{i}\omega\theta}.$$

Following the general framework, we see that $f(\theta) = a_0 + a_\omega f_B(\theta)$, is is sufficient to show that B_n has the eigenvalues

$$\mu^{(1)}_{r_1,j_1,n_\omega(\omega-\beta)} = 2\gamma\cos\left(\theta_{j_1,n_\omega}\right), \qquad r_1 = 1,\ldots,\omega-\beta, \quad j_1 = 1,\ldots,n_\omega, \tag{23}$$

$$\mu^{(2)}_{r_2,j_2,(n_\omega+1)\beta} = 2\gamma\cos\left(\theta_{j_2,n_\omega+1}\right), \qquad r_2 = 1,\ldots,\beta, \quad j_2 = 1,\ldots,n_\omega+1, \tag{24}$$

and that the corresponding eigenvectors

$$\mathbf{x}^{(1)}_{r_1,j_1,n} = \left[x_1^{(r_1,j_1,n)},\ldots,x_n^{(r_1,j_1,n)}\right]^{\mathrm{T}}, \tag{25}$$

$$\mathbf{x}^{(2)}_{r_2,j_2,n} = \left[x_1^{(r_2,j_2,n)},\ldots,x_n^{(r_2,j_2,n)}\right]^{\mathrm{T}}, \tag{26}$$

have components of the form

$$x^{(r_1,j_1,n)}_{\omega(k_1-1)+r_1+\beta} = \gamma^{-k_1}\sin\left(k_1\theta_{j_1,n_\omega}\right), \qquad k_1 = 1,\ldots,n_\omega, \tag{27}$$

$$x^{(r_2,j_2,n)}_{\omega(k_2-1)+r_2} = \gamma^{-k_2}\sin\left(k_2\theta_{j_2,n_\omega+1}\right), \qquad k_2 = 1,\ldots,n_\omega+1, \tag{28}$$

respectively. Because $B_n\mathbf{x} = \mu\mathbf{x}$ for a given eigenpair $(\mu,\mathbf{x})$, for all k the relationships (29)–(33) must hold true. For $\omega \le n/2$

$$\gamma^2 x_{\omega+k} = \mu x_k, \qquad k = 1,\ldots,\omega, \tag{29}$$

$$x_k + \gamma^2 x_{2\omega+k} = \mu x_{\omega+k}, \qquad k = 1,\ldots,n-2\omega, \tag{30}$$

$$x_{n+1-(\omega+k)} = \mu x_{n+1-k}, \qquad k = 1,\ldots,\omega. \tag{31}$$

For $n/2 < \omega < n$

$$\gamma^2 x_{\omega+k} = \mu x_k, \qquad k = 1,\ldots,n-\omega, \tag{32}$$

$$x_{n+1-(\omega+k)} = \mu x_{n+1-k}, \qquad k = 1,\ldots,n-\omega. \tag{33}$$

First we show that equations (29) and (32) are satisfied. For $\mathbf{x}^{(1)}_{r_1,j_1,n}$ in (25) the nonzero components have indices of the form $\omega(k_1-1)+r_1+\beta, k_1 = 1,\ldots,n_\omega$ (as seen in (27)). For $k_1 = 1$ we have $r_1+\beta$ and for $k_2 = 2$ we have $\omega + r_1 + \beta$, which are the only two nonzero components that match (29) and (32), namely

$$x^{(r_1,j_1,n)}_{\omega+r_1+\beta} = \mu^{(1)}_{r_1,j_1,n_\omega(\omega-\beta)} x^{(r_1,j_1,n)}_{r_1+\beta}, \tag{34}$$

or explicitly

$$\gamma^2\gamma^{-2}\sin\left(2\theta_{j_1,n_\omega}\right) = 2\gamma\cos\left(\theta_{j_1,n_\omega}\right)\gamma^{-1}\sin\left(\theta_{j_1,n_\omega}\right), \tag{35}$$

that is

$$\sin\left(2\theta_{j_1,n_\omega}\right) = 2\cos\left(\theta_{j_1,n_\omega}\right)\sin\left(\theta_{j_1,n_\omega}\right),$$

which is true owing to the trigonometric identity

$$\sin\left(2\gamma_1\right) = 2\cos\left(\gamma_1\right)\sin\left(\gamma_1\right). \tag{36}$$

For $\mathbf{x}^{(2)}_{r_2,j_2,n}$ in (26) we observe the same behavior as for $\mathbf{x}^{(1)}_{r_1,j_1,n}$ in (25) above, but the relation analogous to (34) is now

$$x^{(r_2,j_2,n)}_{\omega+r_2} = \mu^{(2)}_{r_2,j_2,(n_\omega+1)\beta} x^{(r_2,j_2,n)}_{r_2}.$$

Namely, it is the same as (35), except for the fact that $\theta_{j_2,n_\omega+1}$ replaces θ_{j_1,n_ω}.

Secondly, we show that (30) is true. For $\mathbf{x}^{(1)}_{r_1,j_1,n}$ in (25) the nonzero components have indices of the form $\omega(k_1-1)+r_1+\beta, k_1 = 1,\ldots,n_\omega$ (as seen in (27)). For k_1, k_1+1, k_1+2, with $k_1 = 1,\ldots,k^{r_1,j_1}_{max}$, where $k^{r_1,j_1}_{max} \le (n-r_1-\beta-\omega)/\omega, k^{r_1,j_1}_{max} \in \mathbb{N}$, we find all nonzero terms of (30) expressed as

$$x^{(r_1,j_1,n)}_{\omega(k_1-1)+r_1+\beta} + \gamma^2 x^{(r_1,j_1,n)}_{\omega(k_1+1)+r_1+\beta} = \mu^{(1)}_{r_1,j_1,n_\omega(\omega-\beta)} x^{(r_1,j_1,n)}_{\omega k_1+r_1+\beta},$$

or explicitly

$$\begin{aligned}\gamma^{-(\omega(k_1-1)+r_1+\beta)}\sin\left(\left(\omega(k_1-1)+r_1+\beta\right)\theta_{j_1,n_\omega}\right)+\\ +\gamma^2\gamma^{-(\omega(k_1+1)+r_1+\beta)}\sin\left(\left(\omega(k_1+1)+r_1+\beta\right)\theta_{j_1,n_\omega}\right)=\\ =2\gamma\cos\left(\theta_{j_1,n_\omega}\right)\gamma^{-(\omega k_1+r_1+\beta)}\sin\left(\left(\omega k_1+r_1+\beta\right)\theta_{j_1,n_\omega}\right),\end{aligned}$$

or

$$\begin{aligned}\sin\left(\left(\omega(k_1-1)+r_1+\beta\right)\theta_{j_1,n_\omega}\right)+\sin\left(\left(\omega(k_1+1)+r_1+\beta\right)\theta_{j_1,n_\omega}\right)=\\ =2\cos\left(\theta_{j_1,n_\omega}\right)\sin\left(\left(\omega k_1+r_1+\beta\right)\theta_{j_1,n_\omega}\right),\end{aligned}$$

which is satisfied because of the trigonometric identity

$$\sin\left(\gamma_1\right)+\sin\left(\gamma_2\right)=2\cos\left(\frac{\gamma_1-\gamma_2}{2}\right)\sin\left(\frac{\gamma_1+\gamma_2}{2}\right).$$

For $\mathbf{x}^{(2)}_{r_2,j_2,n}$ in (26), for $k_2=1,\ldots,k^{r_2,j_2}_{max}$, where $k^{r_2,j_2}_{max}\leq(n-r_2-\omega)/\omega, k^{r_2,j_2}_{max}\in\mathbb{N}$, taking into account (30), we find

$$x^{(r_2,j_2,n)}_{\omega(k_2-1)+r_2}+\gamma^2 x^{(r_2,j_2,n)}_{\omega(k_2+1)+r_1}=\mu^{(2)}_{r_2,j_2,(n_\omega+1)\beta}x^{(r_2,j_2,n)}_{\omega k_2+r_2},$$

and this is proven as for the case $\mu^{(1)}_{r_1,j_1,n_\omega(\omega-\beta)}$ and $\mathbf{x}^{(1)}_{r_1,j_1,n}$ described above.

Lastly we show that (31) and (33) are true. For $\mathbf{x}^{(1)}_{r_1,j_1,n}$ in (25) the nonzero components have indices of the form $\omega(k_1-1)+r_1+\beta, k_1=1,\ldots,n_\omega$ (as seen in (27)). For $k_1=n_\omega$ we have $n+r_1-\omega$ and $k_2=n_\omega-1$ we have $n+r_1-2\omega$, which are the only two nonzero components that match (31) and (33), namely

$$x^{(r_1,j_1,n)}_{n+r_1-2\omega}=\mu^{(1)}_{r_1,j_1,n_\omega(\omega-\beta)}x^{(r_1,j_1,n)}_{n+r_1-\omega},\tag{37}$$

or explicitly

$$\begin{aligned}\gamma^{-(n_\omega-1)}\sin\left((n_\omega-1)\theta_{j_1,n_\omega}\right)&=2\gamma\cos\left(\theta_{j_1,n_\omega}\right)\gamma^{-n_\omega}\sin\left(n_\omega\theta_{j_1,n_\omega}\right),\\ \sin\left((n_\omega-1)\theta_{j_1,n_\omega}\right)&=2\cos\left(\theta_{j_1,n_\omega}\right)\sin\left(n_\omega\theta_{j_1,n_\omega}\right),\\ \sin\left((n_\omega-1)\frac{j_1\pi}{n_\omega+1}\right)&=2\cos\left(\frac{j_1\pi}{n_\omega+1}\right)\sin\left(n_\omega\frac{j_1\pi}{n_\omega+1}\right).\end{aligned}\tag{38}$$

Since

$$\sin\left((n_\omega-1)\frac{j_1\pi}{n_\omega+1}\right)=\sin\left(j_1\pi-2\frac{j_1\pi}{n_\omega+1}\right)=(-1)^{j_1+1}\sin\left(2\frac{j_1\pi}{n_\omega+1}\right)$$

and

$$\sin\left(n_\omega\frac{j_1\pi}{n_\omega+1}\right)=\sin\left(j_1\pi-\frac{j_1\pi}{n_\omega+1}\right)=(-1)^{j_1+1}\sin\left(\frac{j_1\pi}{n_\omega+1}\right),$$

we deduce that relation (38) is equivalent to

$$\sin\left(2\theta_{j_1,n_\omega}\right)=2\cos\left(\theta_{j_1,n_\omega}\right)\sin\left(\theta_{j_1,n_\omega}\right),\tag{39}$$

which is an identity, because of the basic relation in (36). Equivalently, the latter is true for $\mu^{(2)}_{r_2,j_2,(n_\omega+1)\beta}$ in (24) and for $\mathbf{x}^{(2)}_{r_2,j_2,n}$ in (26). □

Example 2. *To continue Example 1, where the sampling grid is computed for $n=5$ and $\omega=3$, we here show the explicit expression of eigenvalues and eigenvectors for a simple example. Take $a_0=2, a_\omega=3$, $a_{-\omega}=7$, that is*

$$A_5=\begin{bmatrix}2&0&0&7&0\\0&2&0&0&7\\0&0&2&0&0\\3&0&0&2&0\\0&3&0&0&2\end{bmatrix},$$

then by using $\tilde{\theta}_n$ defined in Example 1 and Theorem 1 we have $\mu^{(1)}_{j_1,n_\omega}$ and $\mu^{(2)}_{j_2,n_\omega}$ defined by

$$\mu^{(1)}_{1,1} = 2 + 2\sqrt{21}\cos\left(\frac{\pi}{2}\right), \quad \mu^{(2)}_{1,1} = 2 + 2\sqrt{21}\cos\left(\frac{\pi}{3}\right), \quad \mu^{(2)}_{2,1} = 2 + 2\sqrt{21}\cos\left(\frac{2\pi}{3}\right),$$

and the set of all eigenvalues, is thus,

$$\mu_5 = \left\{\mu^{(1)}_{1,1,1}, \mu^{(2)}_{1,1,1}, \mu^{(2)}_{2,1,1}, \mu^{(2)}_{1,2,1}, \mu^{(2)}_{2,2,1}\right\} = \left\{\mu^{(1)}_{1,1}, \mu^{(2)}_{1,1}, \mu^{(2)}_{1,1}, \mu^{(2)}_{2,1}, \mu^{(2)}_{2,1}\right\} = 2 + \sqrt{21}\,\{0, 1, 1, -1, -1\}.$$

An eigenvector for each eigenvalue is computed using Theorem 2

$$\begin{aligned}
\mathbf{x}^{(1)}_{1,1,5} &= \left[0, 0, \sqrt{\frac{3}{7}}\sin\left(\frac{\pi}{2}\right), 0, 0\right]^{\mathrm{T}} = \sqrt{\frac{3}{7}}\,[0, 0, 1, 0, 0]^{\mathrm{T}},\\
\mathbf{x}^{(2)}_{1,1,5} &= \left[\sqrt{\frac{3}{7}}\sin\left(\frac{\pi}{3}\right), 0, 0, \left(\sqrt{\frac{3}{7}}\right)^2\sin\left(\frac{2\pi}{3}\right), 0\right]^{\mathrm{T}} = \frac{\sqrt{3}}{2}\sqrt{\frac{3}{7}}\left[1, 0, 0, \sqrt{\frac{3}{7}}, 0\right]^{\mathrm{T}},\\
\mathbf{x}^{(2)}_{2,1,5} &= \left[0, \sqrt{\frac{3}{7}}\sin\left(\frac{\pi}{3}\right), 0, 0, \left(\sqrt{\frac{3}{7}}\right)^2\sin\left(\frac{2\pi}{3}\right)\right]^{\mathrm{T}} = \frac{\sqrt{3}}{2}\sqrt{\frac{3}{7}}\left[0, 1, 0, 0, \sqrt{\frac{3}{7}}\right]^{\mathrm{T}},\\
\mathbf{x}^{(2)}_{1,2,5} &= \left[\sqrt{\frac{3}{7}}\sin\left(\frac{2\pi}{3}\right), 0, 0, \left(\sqrt{\frac{3}{7}}\right)^2\sin\left(\frac{4\pi}{3}\right), 0\right]^{\mathrm{T}} = \frac{\sqrt{3}}{2}\sqrt{\frac{3}{7}}\left[1, 0, 0, -\sqrt{\frac{3}{7}}, 0\right]^{\mathrm{T}},\\
\mathbf{x}^{(2)}_{2,2,5} &= \left[0, \sqrt{\frac{3}{7}}\sin\left(\frac{2\pi}{3}\right), 0, 0, \left(\sqrt{\frac{3}{7}}\right)^2\sin\left(\frac{4\pi}{3}\right)\right]^{\mathrm{T}} = \frac{\sqrt{3}}{2}\sqrt{\frac{3}{7}}\left[0, 1, 0, 0, -\sqrt{\frac{3}{7}}\right]^{\mathrm{T}}.
\end{aligned}$$

We finally show that $A_n\mathbf{x}^{(1)}_{r_1,j_1,n} = \mu^{(1)}_{r_1,j_1,n_\omega(\omega-\beta)}\mathbf{x}^{(1)}_{r_1,j_1,n}$ and $A_n\mathbf{x}^{(2)}_{r_2,j_2,n} = \mu^{(2)}_{r_2,j_2,(n_\omega+1)\beta}\mathbf{x}^{(2)}_{r_2,j_2,n}$ is true for all $j_1 = 1, \ldots, n_\omega, r_1 = 1, \ldots, \omega - \beta, j_2 = 1, \ldots, n_\omega + 1$, and $r_2 = 1, \ldots, \beta$.

$$\begin{aligned}
A_5\mathbf{x}^{(1)}_{1,1,5} &= \sqrt{\frac{3}{7}}\,[0, 0, 2, 0, 0] = \mu^{(1)}_{1,1,1}\mathbf{x}^{(1)}_{1,1,5},\\
A_5\mathbf{x}^{(2)}_{1,1,5} &= \frac{\sqrt{3}}{2}\sqrt{\frac{3}{7}}\left[2 + \sqrt{21}, 0, 0, 3 + \sqrt{\frac{12}{7}}, 0\right] = \mu^{(2)}_{1,1,1}\mathbf{x}^{(2)}_{1,1,5},\\
A_5\mathbf{x}^{(2)}_{2,1,5} &= \frac{\sqrt{3}}{2}\sqrt{\frac{3}{7}}\left[0, 2 + \sqrt{21}, 0, 0, 3 + \sqrt{\frac{12}{7}}\right] = \mu^{(2)}_{2,1,1}\mathbf{x}^{(2)}_{2,1,5},\\
A_5\mathbf{x}^{(2)}_{1,2,5} &= \frac{\sqrt{3}}{2}\sqrt{\frac{3}{7}}\left[2 - \sqrt{21}, 0, 0, 3 - \sqrt{\frac{12}{7}}, 0\right] = \mu^{(2)}_{1,2,1}\mathbf{x}^{(2)}_{1,2,5},\\
A_5\mathbf{x}^{(2)}_{2,2,5} &= \frac{\sqrt{3}}{2}\sqrt{\frac{3}{7}}\left[0, 2 - \sqrt{21}, 0, 0, 3 - \sqrt{\frac{12}{7}}\right] = \mu^{(2)}_{2,2,1}\mathbf{x}^{(2)}_{2,2,5}.
\end{aligned}$$

2.3 The real symmetric SST Toeplitz case: the generating function and a simplified distribution function

We now consider the previous results from the point of view of spectral distributions in the sense of Weyl. First we introduce some notations and definitions concerning general sequences of matrices. For any function F defined on the complex field and for any matrix A_n of size d_n, by the symbol $\Sigma_\lambda(F, A_n)$, we denote the means

$$\frac{1}{d_n}\sum_{j=1}^{d_n} F[\lambda_j(A_n)].$$

Moreover, given a sequence $\{A_n\}$ of matrices of size d_n with $d_n < d_{n+1}$ and given a Lebesgue-measurable function ψ defined over a measurable set $K \subset \mathbb{R}^\nu$, $\nu\mathbb{N}^+$, of finite e positive Lebesgue measure $\mu(K)$, we say that $\{A_n\}$ is distributed as (ψ, K) in the sense of the eigenvalues if for any continuous F with bounded support the following limit relation holds

$$\lim_{n\to\infty}\Sigma_\lambda(F, A_n) = \frac{1}{\mu(K)}\int_K F(\psi)\,\mathrm{d}\mu. \tag{40}$$

In this case, we write in short $\{A_n\} \sim_\lambda (\psi, K)$. In Remark 3 we provide an informal meaning of the notion of eigenvalue distribution.

Remark 3. *The informal meaning behind the above definition is the following. If ψ is continuous, n is large enough, and*

$$\left\{\mathbf{x}_j^{(m_n)},\ j = 1, \ldots, d_n\right\}$$

is an equispaced grid on K, then a suitable ordering $\lambda_j(A_n)$, $j = 1, \ldots, d_n$, of the eigenvalues of A_n is such that the pairs $\left\{\left(\mathbf{x}_j^{(d_n)}, \lambda_j(A_n)\right),\ j = 1, \ldots, m_n\right\}$ reconstruct approximately the hypersurface

$$\{(\mathbf{x}, \psi(\mathbf{x})),\ \mathbf{x} \in K\}.$$

In other words, the spectrum of A_n 'behaves' like a uniform sampling of ψ over K. For instance, if $\nu = 1$, $d_n = n$, and $K = [a, b]$, then the eigenvalues of A_n are approximately equal to $\psi(a + j(b-a)/n)$, $j = 1, \ldots, n$, for n large enough. Analogously, if $\nu = 2$, $d_n = n^2$, and $K = [a_1, b_1] \times [a_2, b_2]$, then the eigenvalues of A_n are approximately equal to $\psi(a_1 + j(b_1 - a_1)/n, a_2 + k(b_2 - a_2)/n)$, $j, k = 1, \ldots, n$, for n large enough.

Let f be a complex-valued (Lebesgue) integrable function, defined over $Q = (-\pi, \pi)$ and let us consider the sequence $\{T_n(f)\}$ with $T_n(f) = \left(\hat{f}_{j-k}\right)_{j,k=1}^n$, $\hat{f}_s$, $s \in \mathbb{Z}$, being the Fourier coefficients of f defined as in (2). The asymptotic distribution of eigen and singular values of a sequence of Toeplitz matrices has been thoroughly studied in the last century (for example see [7, 22] and the references reported therein). The starting point of this theory, which contains many extensions and other results, is a famous theorem of Szegö [13], which we report in the Tyrtyshnikov and Zamarashkin version [22]:

Theorem 3. *If f is integrable over Q, and if $\{T_n(f)\}$ is the sequence of Toeplitz matrices generated by f, then it holds*

$$\{T_n^*(f)T_n(f)\} \sim_\lambda (|f|^2, Q). \tag{41}$$

Moreover, if f is also real-valued, then each matrix $T_n(f)$ is Hermitian and

$$\{T_n(f)\} \sim_\lambda (f, Q). \tag{42}$$

However, a simple remark has to be added. The symbol is the Weyl sense is far from unique and in fact any rearrangement is still a symbol. A simple case is given by standard Toeplitz sequences, when the symbol f is even that is $f(\theta) = f(-\theta)$ almost everywhere, $\theta \in Q$. In that case, relation (42) is

$$\lim_{n\to\infty} \Sigma_\lambda(F, T_n(f)) = \frac{1}{2\pi} \int_{-\pi}^{\pi} F(f(\theta))\, \mathrm{d}\theta. \tag{43}$$

However, due to the even character of f, we have

$$\int_{-\pi}^{0} F(f(\theta))\, \mathrm{d}\theta = \int_0^{\pi} F(f(\theta))\, \mathrm{d}\theta$$

so that we deduce

$$\lim_{n\to\infty} \Sigma_\lambda(F, T_n(f)) = \frac{1}{\pi} \int_0^{\pi} F(f(\theta))\, \mathrm{d}\theta, \tag{44}$$

that is $\{T_n(f)\} \sim_\lambda (f, Q_+)$, $Q_+ = (0, \pi)$, and in fact the grid points are searched not in the big interval Q but in the restricted interval Q_+ (see Remark 3).

However, formula (20) in Theorem 1 seems to be confusing, since the generating function is $g_\omega(\theta) = a_0 + 2a_\omega \cos(\omega\theta)$, while the eigenvalues result to be an equispaced sampling of the function $a_0 + 2|a_\omega| \cos(\theta)$. Since Theorem 3 tells one that $\{T_n(g_\omega)\} \sim_\lambda (g_\omega, Q)$, while our explicit computation tells one that $\{T_n(g_\omega)\} \sim_\lambda (g_1, Q_+)$, it follows that g_1 on Q_+ is a rearrangement of g_ω on Q.

Indeed, the latter is true, as demonstrated in the following simple derivations:

$$\begin{aligned}
\int_{-\pi}^{\pi} F(g_\omega(\theta))\, \mathrm{d}\theta &= \int_0^{2\pi} F(g_\omega(\theta))\, \mathrm{d}\theta \\
&= \omega \int_0^{2\pi/\omega} F(g_\omega(\theta))\, \mathrm{d}\theta \\
&= \omega \int_0^{2\pi} F(g_\omega(s/\omega))\, \mathrm{d}s/\omega \\
&= \int_0^{2\pi} F(g_1(s))\, \mathrm{d}s = 2\int_0^{\pi} F(g_1(s))\, \mathrm{d}s.
\end{aligned}$$

By the way the fact that g_1 has exactly two branches, one monotonically increasing on $(0, \pi/2)$ and the other monotonically decreasing on $(\pi/2, \pi)$, represents a qualitative confirmation of the fact that the grid $\tilde{\theta}_n$ in (19), for the exact eigenvalue formulae, is obtained by the merging of exactly two distinct grids, $\tilde{\theta}^{(1)}_{n_\omega(\omega-\beta)}$ and $\tilde{\theta}^{(2)}_{(n_\omega+1)\beta}$, independently of the parameter ω.

3 The real symmetric SST case and its use in the general symmetric banded Toeplitz case

Let A_n be a Toeplitz matrix of order n and let $\hat{\omega} < n$ be a positive integer

$$A_n = \begin{bmatrix} a_0 & a_1 & \cdots & a_{\hat{\omega}} & & & & & \\ a_1 & a_0 & \ddots & & \ddots & & & & \\ \vdots & \ddots & \ddots & \ddots & & \ddots & & & \\ a_{\hat{\omega}} & & \ddots & \ddots & \ddots & & \ddots & & \\ & \ddots & & \ddots & \ddots & \ddots & & a_{\hat{\omega}} & \\ & & \ddots & & \ddots & \ddots & \ddots & \vdots & \\ & & & \ddots & & \ddots & a_0 & a_1 & \\ & & & & a_{\hat{\omega}} & \cdots & a_1 & a_0 & \end{bmatrix}, \tag{45}$$

where the coefficients a_k, $k = 0, \ldots, \hat{\omega}$, are real numbers.

We now show that the behavior of the spectrum of such matrices can be qualitatively described via the spectral behavior of two different types of matrices: matrices of the form in (4) with different $\omega = 2, \ldots, \hat{\omega}$ and with $a_0, a_\omega = a_{-\omega}$, real numbers, and matrices of the form (45) with monotone generating function f on $[0, \pi]$, as the case of $f(\theta) = (2 - 2\cos(\theta))^2$. We observe that the case $f(\theta) = (2 - 2\cos(\theta))^2$ corresponds to the choice of $q = 2$ with $a_0 = 6, a_1 = -4, a_2 = 1$ and that for such a case an expansion similar to that in (3) holds. We remind that expansions as in (3) are observed in [2, 9] (and formally proven under mild assumptions [2]) for the general case, in which the generating function is a monotone cosine polynomial in $[0, \pi]$.

In Subsection 3.1, we compare the generating function $g_\omega(\theta) = 2 - 2\cos(\omega\theta)$ with the spectrum of matrices of the form in (4) with different $\omega = 2, \ldots, q$ and with $a_0, a_\omega = a_{-\omega}$, real numbers, by proving the expansions in (47).

In Subsection 3.2, we show numerical evidence that for a general matrix of the form (45) a qualitative comparison between the eigenvalues and the generating function is described by either an expansion like (3), characterizing the monotone case, or expansion like (47), characterizing the purely oscillatory case as $g_\omega(\theta) = 2 - 2\cos(\omega\theta)$, $\omega = 2, \ldots, q$. From a computational viewpoint, as explained in [9], the crucial observation is that such a qualitative behavior turns out to be the theoretical key for designing fast extrapolation-type algorithms for computing eigenvalues of large matrices as in (45).

3.1 The real symmetric SST Toeplitz case: eigenvalues and generating function

Typically a correct symbol and grid combination, which together exactly samples the eigenvalues of a given matrix, is not known but the error can in some cases be reconstructed, see [9].

When approximating the eigenvalues for the standard non-monotone symbol

$$f(\theta) = g_\omega(\theta) = 2 - 2\cos(\omega\theta), \tag{46}$$

with $1 < \omega$ fixed with respect to n, and sampling $g_\omega(\cdot)$ at the standard equispaced grid of (8), we obtain the exact eigenvalues plus an error. This error can be expressed analytically, since the eigenvalues are given by Theorem 1. Subsequently we furnish an expression for the expansion of such an error (refer also to [9] for similar expansions in the monotone case).

We begin by defining the permutations $\pi_n, \sigma_n : \{1, \ldots, n\} \to \{1, \ldots, n\}$ such that $g(\tilde{\theta}_{\pi_n(1),n}) \leq \ldots \leq g(\tilde{\theta}_{\pi_n(n),n})$, $f(\theta_{\sigma_n(1),n}) \leq \ldots \leq f(\theta_{\sigma_n(n),n})$. We denote $\mu_{j,n} = g(\tilde{\theta}_{j,n})$, $\lambda_{j,n} = g(\tilde{\theta}_{\pi_n(j),n})$, and $\nu_{j,n} = f(\theta_{j,n})$, $\xi_{j,n} = g(\theta_{\sigma_n(j),n})$.

The error for (46) with sampling grid (8) to approximate the eigenvalues after sorting is thus

$$E_{j,n} = g(\tilde{\theta}_{\pi_n(j),n}) - f\left(\theta_{\sigma_n(j),n}\right) = \lambda_{j,n} - \xi_{j,n} \tag{47}$$

This error is shown for example in Figure 1(a)–(c) in light gray for $\omega = 3$. At first glance this error can seem chaotic, but it is clear numerically that in this case, and for any $1 < \omega < n$, there will be ω^2 different "error modes"; ω different for each $\beta = \text{mod}(n, \omega) = 0, \ldots, \omega - 1$. For each β we will denote the different error modes by $s = 0, \ldots, \omega - 1$. In Figure 1(a)–(c) these modes are shown for $\beta = 0, 1, 2$, $s = 0$ yellow (dotted),

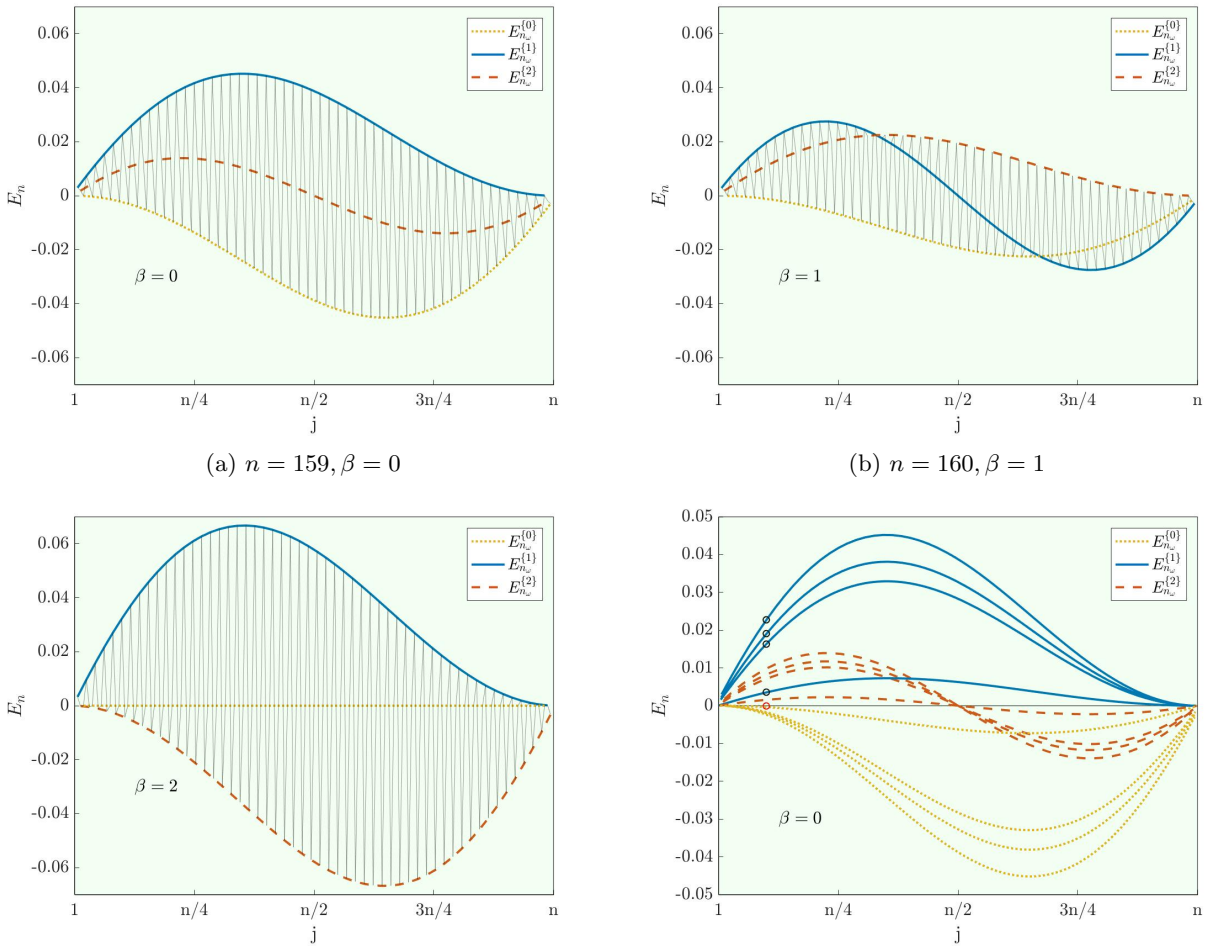

(a) $n = 159, \beta = 0$

(b) $n = 160, \beta = 1$

(c) $n = 161, \beta = 2$

(d) Estimation of $c_{k,0}$, $k = 1, 2, 3$; $\bar{\theta} = \pi/10, \beta = 0$

Figure 1: Errors for eigenvalue approximations for matrices of different sizes with standard symbol $g_3(\theta) = 2 - 2\cos(3\theta)$ and grids $\theta_{j,n} = j\pi h, j = 1, \ldots, n, h = 1/(n+1)$. For each $\beta = \mathrm{mod}(n, \omega) = \mathrm{mod}(n, 3)$ there is $\omega = 3$ different error modes $E_{n_\omega+\eta}^{\{i\}}, i = 0, 1, 2$, represented in yellow (dotted), blue (solid), and red (dashed). In grey is shown the errors not separated into different error modes. In panel (d) is shown the error reduction for $g_3(\theta) = 2 - 2\cos(3\theta)$ for $\bar{\theta} = \pi/10$ using the algorithm presented in [9].

$s = 1$ blue (solid), and $s = 2$ red (dashed). Each error mode for a given n and β is given by the indices $j_s \in I_s, s = 0, \ldots, \omega - 1$, where $I_s = \{s, s + \omega, s + 2\omega, \ldots\}$ (except for $s = 0$ where $I_0 = \{\omega, 2\omega, \ldots\}$), and the union of all I_s is the whole set of indices $\{1, \ldots, n\}$. In other words $s = \mathrm{mod}(j, \omega)$ for $j = 1, \ldots, n$ and for $s = 0$ we have $j_0 = j_\omega \omega$, $j_\omega = 1, \ldots, n_\omega$ and $s > 0$, $j_s = s + (j_\omega - 1)\omega$, $j_\omega = 1, \ldots n_\omega + \eta$, where $n_\omega = (n - \beta)/\omega$ and $\eta = 1$ for $s = 1, \ldots, \beta$ and otherwise $\eta = 0$. In this setting there exist functions $c_{k,s}(\cdot)$, $s = 0, 1, \ldots, \omega - 1, k \geq 1$ for which the error

$$E_{j_s,n} = g(\tilde{\theta}_{\pi_n(j_s),n}) - f\left(\theta_{\sigma_n(j_s),n}\right) = \lambda_{j_s,n} - \xi_{j_s,n} = \lambda_{j_\omega,n_\omega+\eta}^{\{s\}} - \xi_{j_\omega,n_\omega+\eta}^{\{s\}} = E_{j_\omega,n_\omega+\eta}^{\{s\}} \tag{48}$$

has the form

$$E_{j_\omega,n_\omega+\eta}^{\{s\}} = \sum_{k=1}^{\infty} c_{k,s}\left(\theta_{\sigma_n(j_s),n}\right) h^k, \qquad h = \frac{1}{n+1}. \tag{49}$$

We will refer to the functions $c_{k,s}(\theta)$, $k = 1, 2, \ldots$, $s = 0, 1, \ldots, \omega - 1$ as higher order symbols.

Example 3. *As a demonstrative example we will look at the symbol $f_3(\theta) = 2 - 2\cos(3\theta)$. We have $n = 12$ and since $\omega = 3$ we have $\beta = 0$ and $n_\omega = 4$. Since $\beta = 0$ is the simplest case where $\tilde{\theta}_n = \tilde{\theta}_n^{(1)}$, which consists of $\theta_{n_\omega} = \theta_4$ repeated $\omega - \beta = 3$ times. We have*

$$\theta_{j_1,n_\omega} = \frac{j_1\pi}{n_\omega + 1} \quad j_1 = 1, \ldots, n_\omega, \quad \theta_{j,n} = \frac{j\pi}{n+1}, \quad j = 1, \ldots, n.$$

In the following table is shown the different evaluations

j	1	2	3	4	5	6	7	8	9	10	11	12
$f_3(\theta_{j,n}) = \nu_{j,12}$	$\nu_{1,12}$	$\nu_{2,12}$	$\nu_{3,12}$	$\nu_{4,12}$	$\nu_{5,12}$	$\nu_{6,12}$	$\nu_{7,12}$	$\nu_{8,12}$	$\nu_{9,12}$	$\nu_{10,12}$	$\nu_{11,12}$	$\nu_{12,12}$
$g(\tilde{\theta}_{j,n}) = \mu_{j,12}$	$\mu_{1,4}$	$\mu_{1,4}$	$\mu_{1,4}$	$\mu_{2,4}$	$\mu_{2,4}$	$\mu_{2,4}$	$\mu_{3,4}$	$\mu_{3,4}$	$\mu_{3,4}$	$\mu_{4,4}$	$\mu_{4,4}$	$\mu_{4,4}$.

Sorting the evaluations of $g(\tilde{\theta}_{j,n})$ in a non-decreasing order, that is $g(\tilde{\theta}_{\pi_n(j),n})$ we will have the true eigenvalues

$$\lambda_{12} = \{\mu_{4,4}, \mu_{4,4}, \mu_{4,4}, \mu_{3,4}, \mu_{3,4}, \mu_{3,4}, \mu_{2,4}, \mu_{2,4}, \mu_{2,4}, \mu_{1,4}, \mu_{1,4}, \mu_{1,4}\}.$$

Splitting the eigenvalues into the different indices to attain the error modes gives

$$\begin{aligned}
\lambda_4^{\{0\}} &= \{\mu_{4,4}, \mu_{3,4}, \mu_{2,4}, \mu_{1,4}\} = \{\lambda_{j_0,12}\}, && j_0 = 3,6,9,12, \quad s = \mathrm{mod}(j_0,\omega) = 0,\\
\lambda_4^{\{1\}} &= \{\mu_{4,4}, \mu_{3,4}, \mu_{2,4}, \mu_{1,4}\} = \{\lambda_{j_1,12}\}, && j_1 = 1,4,7,10, \quad s = \mathrm{mod}(j_1,\omega) = 1,\\
\lambda_4^{\{2\}} &= \{\mu_{4,4}, \mu_{3,4}, \mu_{2,4}, \mu_{1,4}\} = \{\lambda_{j_2,12}\}, && j_2 = 2,5,8,11, \quad s = \mathrm{mod}(j_2,\omega) = 2.
\end{aligned}$$

Sorting the evaluations of $f(\theta_{j,n})$ in a non-decreasing order, that is $f(\theta_{\sigma_n(j),n})$ we will have the approximations of the eigenvalues

$$\xi_{12} = \{\nu_{9,12}, \nu_{8,12}, \nu_{1,12}, \nu_{10,12}, \nu_{7,12}, \nu_{2,12}, \nu_{11,12}, \nu_{6,12}, \nu_{3,12}, \nu_{12,12}, \nu_{5,12}, \nu_{4,12}\}.$$

Splitting the approximations of the eigenvalues into the different indices to attain the error modes gives

$$\begin{aligned}
\xi_4^{\{0\}} &= \{\nu_{1,12}, \nu_{2,12}, \nu_{3,12}, \nu_{4,12}\} = \{\xi_{j_0,12}\}, && j_0 = 3,6,9,12, \quad s = \mathrm{mod}(j_0,\omega) = 0,\\
\xi_4^{\{1\}} &= \{\nu_{9,12}, \nu_{10,12}, \nu_{11,12}, \nu_{12,12}\} = \{\xi_{j_1,12}\}, && j_1 = 1,4,7,10, \quad s = \mathrm{mod}(j_1,\omega) = 1,\\
\xi_4^{\{2\}} &= \{\nu_{8,12}, \nu_{7,12}, \nu_{6,12}, \nu_{5,12}\} = \{\xi_{j_2,12}\}, && j_2 = 2,5,8,11, \quad s = \mathrm{mod}(j_2,\omega) = 2.
\end{aligned}$$

Hence we have the ω different error modes for $\omega = 3$ and $\beta = 0$ are given by

$$E^{\{0\}}_{j_\omega,n_\omega} = g(\theta_{n_\omega+1-j_\omega,n_\omega}) - f_3(\theta_{j_\omega,n}) = g(\theta_{5-j_\omega,4}) - f_3(\theta_{j_\omega,12}), \qquad j_\omega = 1,\dots,4, \tag{50}$$

$$E^{\{1\}}_{j_\omega,n_\omega} = g(\theta_{n_\omega+1-j_\omega,n_\omega}) - f_3(\theta_{j_\omega+2n_\omega,n}) = g(\theta_{5-j_\omega,4}) - f_3(\theta_{j_\omega+8,12}), \qquad j_\omega = 1,\dots,4, \tag{51}$$

$$E^{\{2\}}_{j_\omega,n_\omega} = g(\theta_{n_\omega+1-j_\omega,n_\omega}) - f_3(\theta_{2n_\omega+1-j_\omega,n}) = g(\theta_{5-j_\omega,4}) - f_3(\theta_{9-j_\omega,12}), \qquad j_\omega = 1,\dots,4, \tag{52}$$

since $\eta = 0$ in (49) for all $s = 0,1,2$, because $\beta = 0$. Using the algorithm presented in [9], we look at a specific eigenvalue of interest $\bar{\theta} = \pi/10$. By this we mean that for a matrix of size n the index of the eigenvalue of interest, when they are sorted in a nondecreasing order, $\bar{j}$, is found by $\pi/10 = \bar{j}\pi/(n+1)$. The error is then specifically $E_{\bar{j},n} = \lambda_{\bar{j},n} - \xi_{\bar{j},n}$ or $E^{\{1\}}_{\bar{j}_\omega,n_\omega}$ since $\beta = 0$ for all n of interest in this example. We look specifically at the pairs $(j_1,n_1) = (16,159), (j_2,n_2) = (19,189), (j_3,n_3) = (22,219)$ and $(j,n) = (100,999)$, which is presented in Figure 1(d). The light green background indicates that the derivative of the symbol changes two times in the region. Other examples of a different number of changes are presented in Figures 2 and 3. They are all in error mode $s = \mathrm{mod}(j,\omega) = 1$, so the error will be as

$$E^{\{1\}}_{j_\omega,n_\omega} = g(\theta_{n_\omega+1-j_\omega,n_\omega}) - f_3(\theta_{j_\omega+2n_\omega,n}) \qquad j_\omega = 1,\dots,n_\omega \tag{53}$$

given by (51). We now look at a specific j_ω, namely $\bar{j}_\omega = (n_\omega+7)/10$. Hence the pairs for each error mode are instead $(\bar{j}_\omega, n_\omega)$, that is $(6,53), (7,63), (8,73)$ and $(34,333)$. We then have explicitly

$$E^{\{1\}}_{\bar{j}_\omega,n_\omega} = g(\theta_{n_\omega+1-\bar{j}_\omega,n_\omega}) - f_3(\theta_{\bar{j}_\omega+2n_\omega,n}) = \sum_{k=1}^{\infty} c_{k,1}\left(\bar{\theta}\right) h^k, \qquad h = \frac{1}{n+1}. \tag{54}$$

and we can analytically express the constants $c_{k,1}(\bar{\theta})$. We have

$$\begin{aligned}
E^{\{1\}}_{\bar{j}_\omega,n_\omega} &= g(\theta_{n_\omega+1-\bar{j}_\omega,n_\omega}) - f_3(\theta_{\bar{j}_\omega+2n_\omega,n})\\
&= g\left(\frac{3\pi}{10}\frac{3n_\omega+1}{n_\omega+1}\right) - f_3\left(\frac{7\pi}{10}\right)\\
&= 2\cos\left(\frac{\pi}{10}\right) - 2\cos\left(\pi\frac{\bar{j}_\omega}{n_\omega+1}\right).
\end{aligned} \tag{55}$$

Explicitly the errors in this example in Figure 1(d), denoted by black circles, are

$$E^{\{1\}}_{6,53} = 2\cos\left(\frac{\pi}{10}\right) - 2\cos\left(\frac{6\pi}{54}\right), \quad E^{\{1\}}_{7,63} = 2\cos\left(\frac{\pi}{10}\right) - 2\cos\left(\frac{7\pi}{64}\right),$$
$$E^{\{1\}}_{8,73} = 2\cos\left(\frac{\pi}{10}\right) - 2\cos\left(\frac{8\pi}{74}\right), \quad E^{\{1\}}_{34,333} = 2\cos\left(\frac{\pi}{10}\right) - 2\cos\left(\frac{34\pi}{334}\right),$$

which is verified numerically to machine precision. The red circle in Figure 1(d) shows the error after applying the algorithm of [9], a reduced from $3.518 \cdot 10^{-3}$ *to* $-2.826 \cdot 10^{-8}$.

By reformulating (55) *we get*

$$E^{\{1\}}_{\bar{j}_\omega, n_\omega} = 2\cos\left(\frac{\pi}{10}\right) - 2\cos\left(\frac{\pi}{10} + \frac{9\pi h}{5(1+2h)}\right), \tag{56}$$

and by Taylor expansion of the error (56) *we can derive exactly the constants* $c_{k,1}$ *in* (54).

$$\begin{aligned}
E^{\{1\}}_{\bar{j}_\omega, n_\omega} &= 2\cos\left(\frac{\pi}{10}\right) - \left(2\cos\left(\frac{\pi}{10}\right) + 2\sum_{k=1}^{\infty} \frac{\cos^{(k)}(\pi/10)}{k!} \left(\frac{9\pi h}{5(1+2h)}\right)^k\right) \\
&= -2\sum_{k=1}^{\infty} \frac{\cos^{(k)}(\pi/10)}{k!} \left(\frac{9\pi}{5}\right)^k h^k \left(\frac{1}{1+2h}\right)^k \\
&= -2\sum_{k=1}^{\infty} \frac{\cos^{(k)}(\pi/10)}{k!} \left(\frac{9\pi}{5}\right)^k h^k \left(\sum_{l=0}^{\infty}(-2h)^l\right)^k \\
&= -2\sum_{k=1}^{\infty} \frac{\cos^{(k)}(\pi/10)}{k!} \left(\frac{9\pi}{5}\right)^k \left(\sum_{l=0}^{\infty}(-2)^l h^{l+1}\right)^k \\
&= 2\sin(\pi/10)\left(\frac{9\pi}{5}\right)\sum_{l=0}^{\infty}(-2)^l h^{l+1} + \\
&\quad + \cos(\pi/10)\left(\frac{9\pi}{5}\right)^2 \left(\sum_{l=0}^{\infty}(-2)^l h^{l+1}\right)^2 - \\
&\quad - \frac{\sin(\pi/10)}{3}\left(\frac{9\pi}{5}\right)^3 \left(\sum_{l=0}^{\infty}(-2)^l h^{l+1}\right)^3 - \\
&\quad \underbrace{- 2\sum_{k=4}^{\infty} \frac{\cos^{(k)}(\pi/10)}{k!} \left(\frac{9\pi}{5}\right)^k \left(\sum_{l=0}^{\infty}(-2)^l h^{l+1}\right)^k}_{\mathcal{O}(h^4).}
\end{aligned} \tag{57}$$

If we find all terms larger than $\mathcal{O}(h^4)$ *of* (56) *we can derive expressions for* $c_{k,1}, k = 1, 2, 3$, *that is*

$$\begin{aligned}
E^{\{1\}}_{\bar{j}_\omega, n_\omega} &= 2\sin(\pi/10)\left(\frac{9\pi}{5}\right) \underbrace{\left(h - 2h^2 + 4h^3 + \sum_{l=3}^{\infty}(-2)^l h^{l+1}\right)}_{h-2h^2+4h^3+\mathcal{O}(h^4)} + \\
&\quad + \cos(\pi/10)\left(\frac{9\pi}{5}\right)^2 \underbrace{\left(h - 2h^2 + \sum_{l=3}^{\infty}(-2)^l h^{l+1}\right)^2}_{h^2-4h^3+\mathcal{O}(h^4)} - \\
&\quad - \frac{\sin(\pi/10)}{3}\left(\frac{9\pi}{5}\right)^3 \underbrace{\left(h + \sum_{l=2}^{\infty}(-2)^l h^{l+1}\right)^3}_{h^3+\mathcal{O}(h^4)} + \mathcal{O}(h^4)
\end{aligned}$$

Thus we have

$$E^{\{1\}}_{j_\omega,n_\omega} = \underbrace{2\sin(\pi/10)\left(\frac{9\pi}{5}\right)}_{c_{1,1}(\bar\theta)\approx 3.49489987} h + \underbrace{\left(-4\sin(\pi/10)\left(\frac{9\pi}{5}\right) + \cos(\pi/10)\left(\frac{9\pi}{5}\right)^2\right)}_{c_{2,1}(\bar\theta)\approx 23.42262738} h^2 + \\ + \underbrace{\left(8\sin(\pi/10)\left(\frac{9\pi}{5}\right) - 4\cos(\pi/10)\left(\frac{9\pi}{5}\right)^2 - \frac{\sin(\pi/10)}{3}\left(\frac{9\pi}{5}\right)^3\right)}_{c_{3,1}(\bar\theta)\approx -126.29647972} h^3 + \sum_{k=4}^{\infty} c_{k,1}(\bar\theta)h^k \qquad (58)$$

Note that the explicit expressions of (58) *can be derived for any combination of* n, ω *and* $\bar\theta$*, but will be more complicated if* $\beta > 0$ *since also* $\tilde\theta^{(2)}$ *has to be considered.*

In Table 1 we show the results using the algorithm of [9] to approximate m *different constants* $c_{k,1}(\bar\theta)$ *with the same number of different coarse matrices. As* m *increases,* $\tilde c_{k,1}(\bar\theta)$ *converges to* $c_{k,1}(\bar\theta)$ *as expected. Using the analytical expression of* $c_{k,1}(\bar\theta)$ *in* (58) *we have* $\sum_{k=1}^{3} c_{k,1}(\bar\theta)h^k = 3.51819620 \cdot 10^{-3}$ *and thus the error after the error reduction is* $E^{\{1\}}_{34,333} - \sum_{k=1}^{m} c_{k,1}(\bar\theta)h^k = 3.67020511 \cdot 10^{-10}$.

Table 1: Analytical $c_{k,1}(\bar\theta)$, and the respective approximation $\tilde c_{k,1}(\bar\theta)$, for m different coarse matrices in algorithm from [9] for $g_3(\theta) = 2 - 2\cos(3\theta), \bar\theta = \pi/10$.

	$m=1$	$m=2$	$m=3$	$m=4$
	159	159, 189	159, 189, 219	159, 189, 219, 249
$c_{1,1}(\bar\theta)$	3.49489987	3.49489987	3.49489987	3.49489987
$\tilde c_{1,1}(\bar\theta)$	3.63644656	3.49891734	3.49495321	3.49490028
$c_{2,1}(\bar\theta)$		23.42262738	23.42262738	23.42262738
$\tilde c_{2,1}(\bar\theta)$		22.00467555	23.39212062	23.42229454
$c_{3,1}(\bar\theta)$			−126.29647972	−126.29647972
$\tilde c_{3,1}(\bar\theta)$			−120.50951417	−126.19491717
$E^{\{1\}}_{34,333}$	$3.51819657 \cdot 10^{-3}$	$3.51819657 \cdot 10^{-3}$	$3.51819657 \cdot 10^{-3}$	$3.51819657 \cdot 10^{-3}$
$\sum_{k=1}^{m} \tilde c_{k,1}(\bar\theta)h^k$	$3.63644656 \cdot 10^{-3}$	$3.52092202 \cdot 10^{-3}$	$3.51822482 \cdot 10^{-3}$	$3.51819673 \cdot 10^{-3}$
$E^{\{1\}}_{34,333} - \sum_{k=1}^{m} \tilde c_{k,1}(\bar\theta)h^k$	$-1.18249995 \cdot 10^{-4}$	$-2.72544868 \cdot 10^{-6}$	$-2.82554797 \cdot 10^{-8}$	$-0.16133076 \cdot 10^{-9}$

In Table 2 is shown results using the algorithm from [9] on the nonmonotone cases $g_\omega(\theta) = 2 - 2\cos(\omega\theta)$ *for* $\omega = 2, 3, 4$ *to reduce the error of the eigenvalue approximation on a fine matrix. Presented is the errors for* $m = 0, 1, 2, 3$ *different coarse matrices used to approximate the constants* $c_{k,1}(\bar\theta)$*,* $k = 1, \ldots, m$*. For* $g_2(\theta)$ *the coarse matrices are* $n \in \{149, 189, 209\}$ *and* $n = 9999$*; for* $g_3(\theta)$ *the coarse matrices are* $n \in \{159, 189, 219\}$ *and* $n = 10009$*; for* $g_4(\theta)$ *the coarse matrices are* $n \in \{169, 209, 249\}$ *and* $n = 10009$*. The errors behave as expected and the algorithm from [9] fan thus also in some cases be used for nonmonotone cases, although these examples can be evaluated exactly by the symbol and samplig grid described in Section 2.*

Table 2: Errors for eigenvalue approximations for matrices with standard symbol $g_\omega(\theta) = 2 - 2\cos(\omega\theta), \bar\theta = \pi/10$.

		$E^{\{1\}}_{j_\omega,n_\omega} - \sum_{k=1}^{m} \tilde c_{k,1}(\bar\theta)h^k$		
$g_\omega(\theta)$	$E^{\{1\}}_{j_\omega,n_\omega}$	$m=1$	$m=2$	$m=3$
$g_2(\theta)$	$-3.88581714 \cdot 10^{-5}$	$4.32478954 \cdot 10^{-6}$	$-5.21177503 \cdot 10^{-8}$	$-1.12193334 \cdot 10^{-9}$
$g_3(\theta)$	$34.97240870 \cdot 10^{-5}$	$-13.92056931 \cdot 10^{-6}$	$-38.76938472 \cdot 10^{-8}$	$-5.03491210 \cdot 10^{-9}$
$g_4(\theta)$	$65.96546126 \cdot 10^{-5}$	$-7.93740842 \cdot 10^{-6}$	$-127.70747416 \cdot 10^{-8}$	$-50.14789443 \cdot 10^{-9}$

3.2 The general symmetric banded case: conjectures and numerics

As seen in the previous subsection, given a positive integer $\omega \geq 2$ and the nonmonotone symbol $f(\theta) = g_\omega(\theta) = 2 - 2\cos(\omega\theta)$, and evaluating with a equidistant grid such as $\theta_{j,n} = j\pi h, j = 1, \ldots, n, h = 1/(n+1)$, numerical tests show that the error $E_n = \lambda_n - \xi_n$ can be separated into ω different types of error modes for each $\beta = \text{mod}(n, \omega)$. That is, for each $\beta = \text{mod}(n, \omega)$ there are ω disjoint subgrids of the original grid (see Figure 1 for $\omega = 3$ and the related caption). Each error mode for a given n and β is given by indices $j \in I_s, s = 0, \ldots, \omega - 1$, where $I_0 = \{\omega, 2\omega, 3\omega, \ldots\}$ and for $s > 0$, $I_s = \{s, s+\omega, s+2\omega, \ldots\}$, and the union of all I_s is the whole set of indices $\{1, \ldots, n\}$.

This induces the conjecture that the number of the different expansions is related to the number of sign changes of the derivative of the generating function in the basic interval $(0, \pi)$, that is formulas like

$$\lambda_{j,n} = f(\theta_{\sigma_n(j),n}) + \sum_{k=1}^{m} c_{k,s}\left(\theta_{\sigma_n(j),n}\right) h^k + O(h^{m+1}), \quad j \in I_s \quad s = 0, \ldots, \omega - 1, \tag{59}$$

must hold.

In Figure 2 we see a clarifying example of the nonmonotone error given by the function $f(\theta) = 2 - 2\cos(\theta) - 2\cos(2\theta)$.

In Figure 2(a) is shown the true eigenvalues (sorted, solid in red) and the sampling of the symbol (unsorted, dashed in black). The two different regions displayed in light colors (red on bottom and yellow on top) represents the different number of sign changes in the derivative of the symbol $f(\theta)$ inside the region (zero and one). These different regions will give rise to different characteristics of the behavior of the errors.

The approximation error of the function has the monotone behavior of $(2-2\cos(\theta))^2$, when using for example the grid $(j-1)\pi/(n-1)$ instead of the exact $j\pi/(n+1)$, in the interval $[0, \pi/3]$ with $f(\pi/3) = 2$, and almost the behavior of $2 - 2\cos(2\theta)$ in the interval $[\pi/3, \pi]$ with $f(\pi/3) = f(\pi) = 2$. Indeed, for the eigenvalues belonging to $(-2, 2]$, $-2 = f(0) = \min\ f$, $2 = f(\pi/3)$, as represented in the light red regions of Figure 2, the behavior of the error is like the one related with a monotone function that is (59) with $\omega = 1$ holds. For the eigenvalues belonging to $(2, 17/4)$, $2 = f(\pi/3) = f(\pi)$, $17/4 = \max\ f$, as represented in the light yellow regions in Figure 2, the behavior of the error behaves almost like the one displayed in (59) with $\omega = 2$, since the sign of the derivative changes once.

In Figure 2(b) we present a visualization of error reduction for $f(\theta) = 2 - 2\cos(\theta) - 2\cos(2\theta)$, $\bar{\theta} = \pi/10$ with the algorithm presented in [9]. The fine grid $n = 669$, and the coarse grids are $n \in \{109, 129, 149\}$. The black circles represent the error of symbol approximation on the respective grids and the red circle is the error on the fine grid after reduction using the coarse errors. The error is reduced from $-7.899 \cdot 10^{-4}$ to $-9.959 \cdot 10^{-11}$. Note that here the x axis is ordered by the size of the true eigenvalues. The error left region (light red) behaves like a monotone symbol, whereas the right region (light yellow) behaves in general terms as a symbol of the form g_ω but with a slight shift.

As seen in Figures 2(c–d) the local change is somewhat drastic with a small change of n, but the general structure of the error remains as n increases. In Figure 2(c) we see the errors for $n = 200$ (solid) and $n = 202$ (dashed). Assuming two error modes for each n. Note the rather large "shift" of the error curve just increasing n by two. Note also that the x axis is ordered by n, and not the size of the true eigenvalues. Figure 2(d) we see the errors for $n = 500$ assuming two error modes. Note the general regularity of the error in the large eigenvalues (right part of the figure) is comparable to $n = 200$ and $n = 202$ shown in Figure 2(c). In other words, the global error behavior is still regular in a weaker sense, and should be investigated formally.

In Figure 3 is shown the case of the error using the standard grid on the symbol $f(\theta) = 2 - 2\cos(3\theta) - 2\cos(4\theta)$. In Figure 3(a) the true eigenvalues (sorted, solid red) and the sampling of the symbol (unsorted, dashed black) is shown. Clearly four different regions are present, colored in light red, green, blue, and yellow, depending on the number of sign changes of the derivative of the symbol in the region (zero, two, three, and one). These different regions will give rise to different characteristics of the behavior of the errors.

The error $E_{j,n} = \lambda_{j,n} - f(\theta_{\sigma_n j,n})$, for $n = 1000$, plotted as if there are two error modes, that is $j_1 = 1, 3, 5, \ldots$ (blue) and $j_2 = 2, 4, 6, \ldots$ (red). The light red (first) region shows the error behaving as in the monotone case, that is the error can be reconstructed in the manner presented in [9]. The light yellow (fourth) part shows a clear regularity when representing the error in two sets (blue and red). Although when increasing n we do not just decrease the error in the region but keep the error function, but we also change the number of "peaks", as previously demonstrated in Figure 2. In the light red region the error behaves like for a monotone symbol and the error can be efficiently be reconstructed by the same techniques as described in Section 3.1 and in Figures 1 and 2. The light green (second) and blue (third) regions show "chaotic" behavior, resulting from the "naive" ordering of the approximated eigenvalues. Again this behavior merits further study.

4 Conclusions and future work

The paper contains two types of theoretical results and a numerical part.

The first result concerns the fact that for the SST Toeplitz matrices as in (4), with $a_0, a_\omega, a_{-\omega} \in \mathbb{C}$, $0 < \omega < n$, the eigenvalues and the eigenvectors have a closed form expression. In particular, the formula for the eigenvalues $\mu_{j,n}$ in Theorem 1 is expressed in an elegant and compact way, since the exist a grid $\tilde{\theta}_n$, the one defined in (19), and the simple function $g(\theta) = a_0 + 2\sqrt{a_\omega a_{-\omega}}\cos(\theta)$ such that

$$\mu_{j,n} = g\left(\tilde{\theta}_{j,n}\right), \quad j = 1, \ldots, n.$$

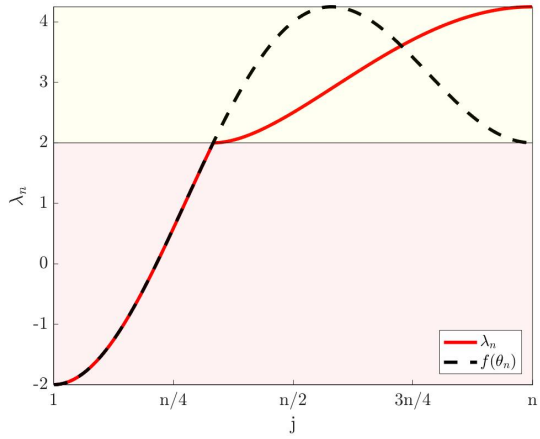

(a) True eigenvalues (sorted, solid in red). Sampling of the symbol (unsorted, dashed in black).

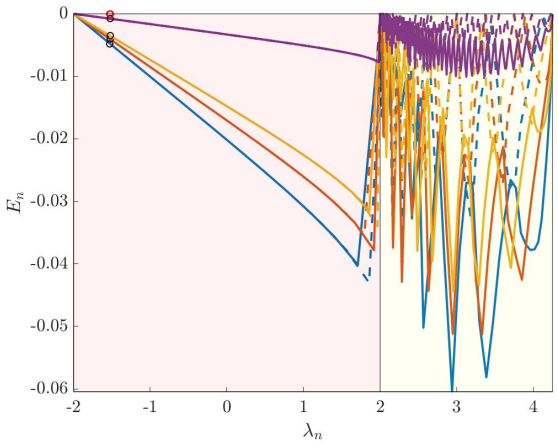

(b) Errors for for different n. Reduction of error for $\bar{\theta} = \pi/10$.

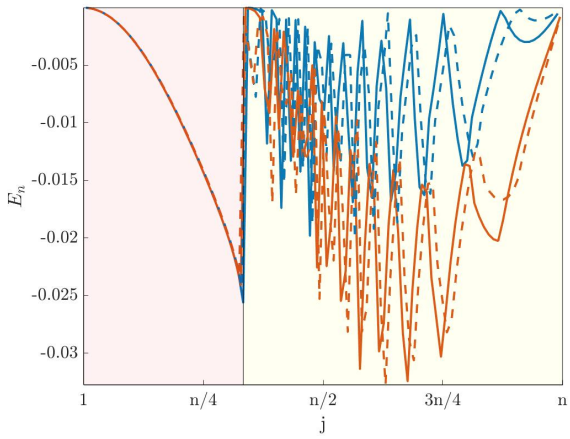

(c) Errors for $n = 200$ (solid) and $n = 202$ (dashed).

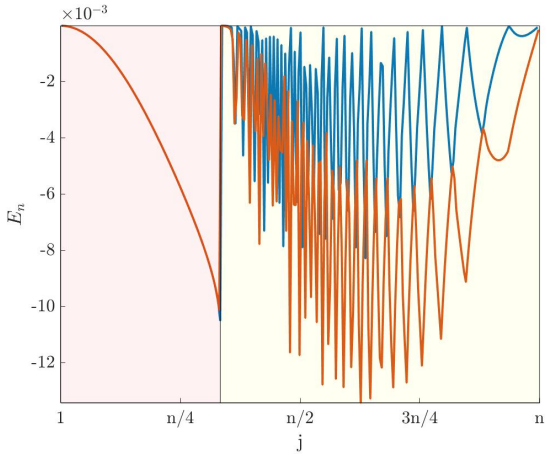

(d) Errors for $n = 500$.

Figure 2: Eigenvalues, symbol, and errors for matrices with standard symbol $f(\theta) = 2 - 2\cos(\theta) - 2\cos(2\theta)$ and grids $\theta_{j,n} = j\pi h, j = 1, \ldots, n, h = 1/(n+1)$.

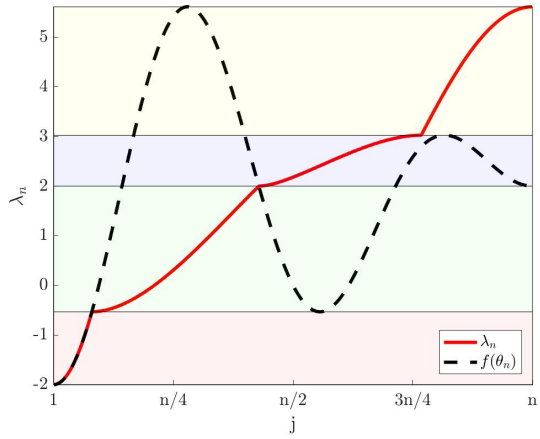

(a) True eigenvalues (sorted, solid in red). Sampling of the symbol (unsorted, dashed in black).

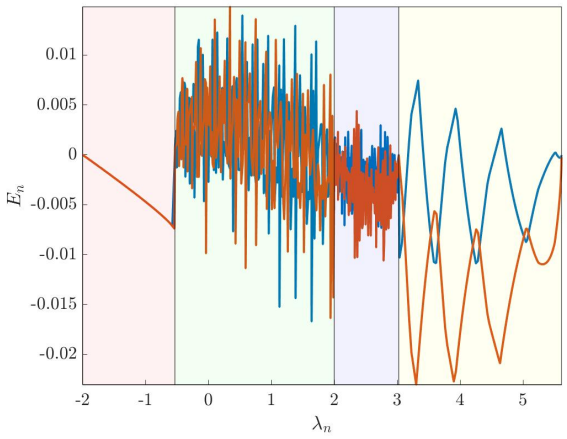

(b) Errors for $n = 1000$.

Figure 3: Eigenvalues, symbol, and errors for a matrix with standard symbol $f(\theta) = 2 - 2\cos(3\theta) - 2\cos(4\theta)$ and grids $\theta_{j,n} = j\pi h, j = 1, \ldots, n, h = 1/(n+1)$.

Furthermore, using basic changes of variable in the integral representation of the distribution results, we show clear relationships between the symbol g and the standard generating functions of the matrices A_n, A_n^{sym}, that is $f_\omega(\theta) = a_0 + a_\omega e^{\mathbf{i}\omega\theta} + a_{-\omega} e^{-\mathbf{i}\omega\theta}$, $g_\omega(\theta) = a_0 + 2\sqrt{a_\omega a_{-\omega}}\cos(\omega\theta)$, respectively. Also, a closed form formula

for the corresponding eigenvectors is presented in Theorem 2.

The second result regards three banded Toeplitz matrices (4), with $a_0, a_\omega, a_{-\omega} \in \mathbb{R}$, $0 < \omega < n$: here we show that an asymptotic expansion of the eigenvalues holds, with respect to the standard generating function and the usual grid (see formula (47)). The latter extends a similar asymptotic expansion holding for the eigenvalues of general symmetric real Toeplitz matrices, having polynomial cosine generating function, which is monotone on $[0, \pi]$ (see formula (3) and [2, 5, 9, 10]): an important example of such matrices are represented by the Finite Difference discretization of the operators $(-1)^q \frac{\partial^{2q}}{\partial x^{2q}}$, whose generating function is $(2 - 2\cos(\theta))^q$, $q \geq 1$.

The final part concerns a conjecture supported by numerical tests in which it is shown that for a generic banded real symmetric Toeplitz matrix, the eigenvalue $\lambda_{j,n}$ compared with $f\left(\theta_{\sigma_n j,n}\right)$ shows either an expansion like formula (47) if $\lambda_{j,n} \in [m, M]$ and $f'(\theta)$ has ω changes of sign for $f(\theta) \in [m, M]$, or it shows an expansion like formula (3) if $\lambda_{j,n} \in [m, M]$ and $f(\theta) \in [m, M]$ is monotone.

The latter gives the ground for extrapolation techniques [8] for computing the eigenvalues of large banded real symmetric Toeplitz matrices in a fast way. Of course, also the multidimensional and the block cases should be considered and explored in a future work, owing to their importance in the numerical approximation of (systems of) partial differential equations.

Acknowledgements

Thanks to family, colleagues, and friends for fruitful discussions and insights. The research of the first author is funded by the Graduate School in Mathematics and Computing (FMB) and Uppsala University, and the second author is supported by the Italian Group of Scientific Computing INDAM-GNCS.

References

[1] D. Bini and M. Capovani, "Spectral and computational properties of band symmetric Toeplitz matrices", *Linear Algebra Appl.*, **52/53** (1983), pp. 99–126.

[2] J. Bogoya, A. Böttcher, S. Grudsky, and E. Maximenko, "Eigenvalues of Hermitian Toeplitz matrices with smooth simple-loop symbols. *J. Math. Anal. Appl.*, **422-2** (2015), pp. 1308–1334.

[3] J. Bogoya, A. Böttcher, and E. Maximenko,"From convergence in distribution to uniform convergence", *Bol. Soc. Mat. Mex.*, **3-22** (2016), pp. 695–710.

[4] J. Bogoya, S. Grudsky, and E. Maximenko, "Eigenvalues of Hermitian Toeplitz matrices generated by simple-loop symbols with relaxed smoothness", *Oper. Theory Adv. Appl.*, **259** (2017), pp. 179–212.

[5] A. Böttcher, S. Grudsky, and E. Maximenko,"Inside the eigenvalues of certain Hermitian Toeplitz band matrices", *J. Comput. Appl. Math.*, **233-9** (2010), pp. 2245–2264.

[6] A. Böttcher and S. Grudsky, *Spectral Properties of Banded Toeplitz Matrices*. SIAM, 2005

[7] A. Böttcher and B. Silbermann, *Introduction to Large Truncated Toeplitz Matrices*. Springer-Verlag, New York 1999.

[8] C. Brezinski and M. Redivo Zaglia, *Extrapolation Methods. Theory and Practice*. Studies in Computational Mathematics, 2. North-Holland Publishing Co., Amsterdam 1991.

[9] S.-E. Ekström, C. Garoni, and S. Serra-Capizzano, "Are the eigenvalues of banded symmetric Toeplitz matrices known in almost closed form?", *Exp. Math.*, in press.

[10] S.-E. Ekström and S. Serra-Capizzano, "Eigenvalues of banded symmetric Toeplitz matrices are known almost in close form?", *TR Division of Scientific Computing, IT Dept, Uppsala U.*, **17** (September 2016): http://www.it.uu.se/research/publications/reports/2016-017/

[11] J.F. Elliott, "The characteristic roots of certain real symmetric matrices." Master's Thesis, University of Tennessee, (1953). http://trace.tennessee.edu/utk_gradthes/2384

[12] F.R. Gantmakher, and M.G. Krein, *Ostsilliatsionnye matritsy i iadra i malye kolebaniia mekhanicheskikh sistem.* Gostekhizdat (Oscillation Matrices and Kernels and Small Vibrations of Mechanical Systems), 1950.

[13] U. Grenander and G. Szegö, *Toeplitz Forms and Their Applications.* Second Edition, Chelsea, New York, 1984.

[14] S. Noschese, L. Pasquini, and L. Reichel, "Tridiagonal Toeplitz matrices: properties and novel applications," *Numer. Linear Algebra Appl.*, **20-2** (2013), pp. 302–326.

[15] S. Serra-Capizzano, "On the extreme eigenvalues of Hermitian (block) Toeplitz matrices", *Linear Algebra Appl.*, **270** (1998), pp. 109–129.

[16] S. Serra-Capizzano, "On the extreme spectral properties of Toeplitz matrices generated by L1 functions with several minima/maxima", *BIT*, **36-1** (1996), pp. 135–142.

[17] S. Serra-Capizzano, D. Bertaccini, and G. Golub, "How to deduce a proper eigenvalue cluster from a proper singular value cluster in the nonnormal case", *SIAM J. Matrix Anal. Appl.*, **27-1** (2005), pp. 82–86.

[18] G.D. Smith, Numerical Solution of Partial Differential Equations: Finite Difference Methods. Second Edition, Clarendon Press, Oxford, 1978

[19] E.M. Stein and G. Weiss, Introduction to Fourier Analysis on Euclidean Spaces. Princeton University Press, Princeton NJ, 1971.

[20] P. Tilli, "A note on the spectral distribution of Toeplitz matrices", *Linear Multil. Algebra,* **45-2/3** (1998), pp.147–159.

[21] E. Tyrtyshnikov, "A unifying approach to some old and new theorems on distribution and clustering", *Linear Algebra Appl.*, **232** (1996), pp. 1–43.

[22] E. Tyrtyshnikov and N. Zamarashkin, "Spectra of multilevel Toeplitz matrices: advanced theory via simple matrix relationships", *Linear Algebra Appl.*, **270** (1998), pp. 15–27.